(2)

ARMY RESEARCH LABORATORY

Time-Temperature Shift Factors for Gun Propellants

Robert J. Lieb
Michael G. Leadore

ARL-TR-131 May 1993

NOTICES

Destroy this report when it is no longer needed. DO NOT return it to the originator.

Additional copies of this report may be obtained from the National Technical Information Service, U.S. Department of Commerce, 5285 Port Royal Road, Springfield, VA 22161.

The findings of this report are not to be construed as an official Department of the Army position, unless so designated by other authorized documents.

The use of trade names or manufacturers' names in this report does not constitute indorsement of any commercial product.

REPORT DOCUMENTATION PAGE

Form Approved
OMB No 0704-0188

1. AGENCY USE ONLY *(Leave blank)*	2 REPORT DATE	3 REPORT TYPE AND DATES COVERED
	May 1993	Final Jun 92 - Oct 92

4. TITLE AND SUBTITLE

Time-Temperature Shift Factors for Gun Propellants

5. FUNDING NUMBERS

PR: 1L161102AH43

6. AUTHOR(S)

Robert J. Lieb and Michael G. Leadore

7. PERFORMING ORGANIZATION NAME(S) AND ADDRESS(ES)

U.S. Army Research Laboratory
ATTN: AMSRL-WT-PE
Aberdeen Proving Ground, MD 21005-5066

8. PERFORMING ORGANIZATION REPORT NUMBER

9. SPONSORING/MONITORING AGENCY NAMES(S) AND ADDRESS(ES)

U.S. Army Research Laboratory
ATTN: AMSRL-OP-CI-B (Tech Lib)
Aberdeen Proving Ground, MD 21005-5066

10. SPONSORING/MONITORING AGENCY REPORT NUMBER

ARL-TR-131

11. SUPPLEMENTARY NOTES

12a. DISTRIBUTION/AVAILABILITY STATEMENT

Approved for public release; distribution is unlimited.

12b. DISTRIBUTION CODE

13. ABSTRACT *(Maximum 200 words)*

To estimate the response of gun propellants at higher rates than can be easily reached within the laboratory, stress relaxation measurements have been made in compression for single- (M14), double- (JA2), and triple-based (M30) propellants, as well as a nitramine composite (M43) gun propellant, over the temperature range of -40 to 60 degrees celcius. Master curves were generated and shift factors were calculated which were used to determine the time-temperature shift factors for each of the propellants over these temperatures.

14. SUBJECT TERMS

Mechanical response, propellants, bed, M30, JA2, M43, stress profile, relaxation

15. NUMBER OF PAGES

27

16. PRICE CODE

17. SECURITY CLASSIFICATION OF REPORT	18. SECURITY CLASSIFICATION OF THIS PAGE	19. SECURITY CLASSIFICATION OF ABSTRACT	20. LIMITATION OF ABSTRACT
UNCLASSIFIED	UNCLASSIFIED	UNCLASSIFIED	SAR

TABLE OF CONTENTS

LIST OF FIGURES

LIST OF TABLES

INTENTIONALLY LEFT BLANK.

1. INTRODUCTION

The response of gun propellant to mechanical stress plays a critical role in the evolution of pressure during the ballistic cycle. Attempts to link the relationship between mechanical measurements performed in the lab and both gun performance and vulnerability have made considerable progress in the last year[1,2,3]. Previous work has revealed that at low temperatures the change in magnitude of failure parameters measured on a single propellant grain correlated well with the change in magnitude of the explosive response of propellant beds upon impact with shaped charge jets[2,3]. However, the mechanical response measurements were performed at rates of about 100 s^{-1} whereas the rate of mechanical deformation during the jet interaction is estimated to be between 10^4 and 10^6 s^{-1}. A more accurate correlation might be obtained if the mechanical response of the material could be more closely determined at higher rates.

One method used to estimate mechanical responses of materials at rates outside the limits of available equipment is to employ the time-temperature superposition principle[4,5] and determine the shift factors for the material using relaxation measurements. These measurements were performed on four propellant types, a single- (M14), double- (JA2), and triple-based (M30) propellants, and a nitramine composite (M43) gun propellant. These propellants were chosen so that a broad range of propellant types would be represented. Since the temperature range of interest for guns is -40 to 60°C, and testing can be easily performed within this range, measurements were made between these temperatures.

From the shift factors measured here, failure parameters can be determined that more accurately correspond to the mechanical response at higher rates. This is accomplished by testing the propellant at appropriately lower temperature. For example, a shift in strain rate by a factor of 100 can be approximated by a temperature shift of -20°C for M14 propellant, as is shown in this report.

2. EXPERIMENTAL PROCEDURE AND RESULTS

2.1 <u>Description of the Tester and Procedure</u>. The propellant relaxation response was measured using a specially designed servohydraulic tester[6], illustrated in Figure 1. The machine allows for compression measurements to be performed at rates of up to 1000 s^{-1} for a specimen with a nominal length of 1 cm. Compression is arrested when contact occurs between the impact bell and cone. Therefore, the amount of specimen compression can be adjusted by setting the anvil height. This contact not only stops the specimen compression, but it also shunts the force around the specimen. The nitrogen spring absorbs and spreads out in time the decelerating force of the ram. The force

applied to the specimen is measured using the gage inside the impact bell. During normal compressive response measurements, displacement is measured with a linear variable differential transformer (LVDT) in the actuator column and is corrected for machine stiffness.

The specimens were prepared from multiperforated gun propellant grains whose formulations are listed in Table 1. A typical 7-perforated specimen appears on the left hand side of Figure 1. Specimen preparation in the relaxation procedure began by cutting the sample with a diamond saw to a length of 1.00 cm. The ends were cut flat, parallel and perpendicular to the grain axis according to the specifications found in a proposed NATO draft STANAG entitled "Uniaxial Compressive Test," which is an updated version of the test entitled "Uniaxial Compressive Gun Propellant Test" found in CPIA Pub 21. Temperature conditioning was achieved by placing prepared grains inside the environmental chamber for a time at least twice that needed to reach thermal equilibrium (30 minutes in most cases). The specimen was then placed on the anvil and tested. This testing took place within the conditioning chamber, so no transfer was required and, therefore, no thermal disruption occurred.

The strain at which relaxation occurred was determined by the distance between the anvil and the force gage when the bell and cone surfaces were mated. That distance was determined by placing a lead specimen on the anvil and performing a compression. The percentage strain used in these tests

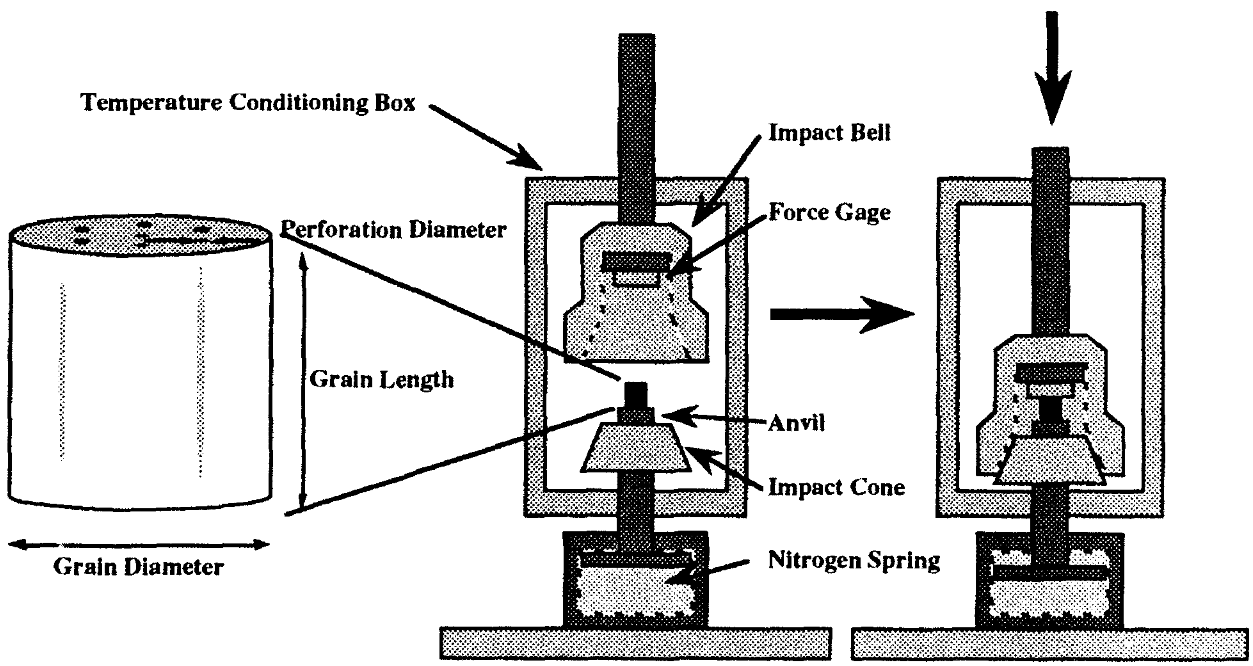

Figure 1. Servohydraulic Stress Relaxation Tester

Table 1. Nominal Percent Composition of Propellants

Component	M14	JA2	M30	M43
Nitrocellulose (NC)	89	59	28	4
NC Nitration Level	12.6	13.1	12.6	12.6
Nitroglycerin (NG)		15	22	
Nitroguanidine (NQ)			48	
Ethyl Centralite (EC)			2	
Diethylene Glycol Dinitrate		25		
Akardit II		1		
RDX (Ground)				76
Cellulose Acetate Butyrate				12
Plasticizer				8
DNT	8			
DBP	2			
DPA	1			

was based on previous mechanical response measurements, and was selected to keep the specimen strain below that at which failure was known to occur. Table 2 gives the average strain to which the propellants were taken during the relaxation measurements.

Once all the conditions for the test were set, the relaxation measurements were made at -40, -20, 0, 20, and 60°C (50°C for JA2). The specimen strain rate was chosen to be $1.00\ s^{-1}$. Data was acquired at a rate 100 points per second for about 40 seconds. Five repetitions were performed for each test condition.

2.2 Test Results. The modulus was calculated by dividing the force by the net area of the specimen to get the stress and then dividing the stress by the strain, determined as described above. A period equal to 10 times the period of compression was removed from the beginning of each relaxation curve to assure that no dynamic effects were in process when data was taken, e.g., four hundredths of a second is the time needed to compress a specimen to four percent. The five Relaxation Modulus-vs-Time curves were then averaged to produce a single curve for

Table 2. Average Specimen Strain

Propellant	Strain
M14	3 %
JA2	5 %
M30	5 %
M43	2 %

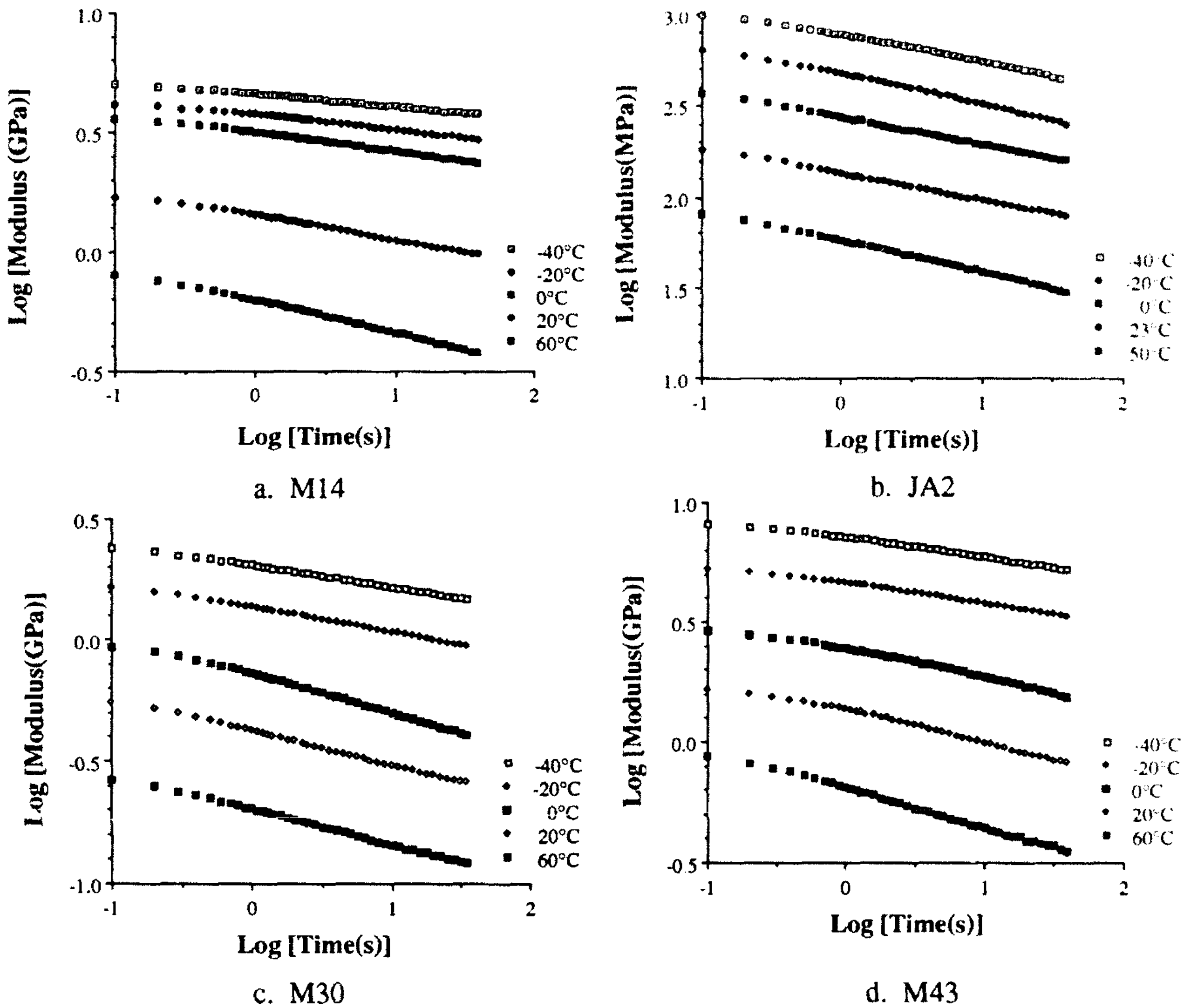

Figure 2. Log Relaxation Modulus vs Log Time for Each Propellant

each propellant at each temperature. These results appear in Figure 2 and are plotted in the usual log-log fashion. Figure 3 provides an example of scatter among data sets collected under the same conditions. All the sources of this scatter are not known. However, the largest source almost certainly arises from error in the strain measurement. At such low strains, small errors make large differences.

3. ANALYSIS

3.1 Master Curve Generation. A master curve was generated from each family of curves presented in Figure 2 by horizontally shifting each of the curves except one, the reference curve, to form a single curve on an expanded time axis. If the curves are to be used for the prediction of relaxation moduli or related phenomena at different rates, then temperature and density compensa-

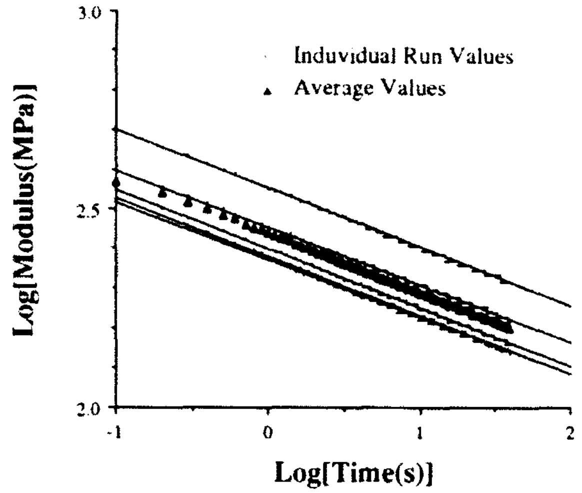

Figure 3. JA2 Relaxation Data at 0°C (as in Figure 2) Showing Typical Scatter about Averaged Values

tion are required[4,5], since the modulus and density of the material are a function of the temperature. However, the primary interest in these calculations is to know the temperature at which testing can be performed that would simulate higher rate conditions. For this latter purpose no temperature correction is required because the testing will occur at the lower temperature and the amount of shift has already accounted for moduli differences. Master curves for temperature compensated calculations appear in Appendix I. No compensation for density changes was made, since the differences in density at the temperatures used here are small. The amount that each of the curves is shifted can be used to establish the relationship between the temperature corresponding to that curve and the time (rate) with respect to the unshifted curve. Since this shift takes place on a log scale, the amount of shift corresponds to a rate factor.

The method used to shift the curves is illustrated in Figure 4 and is explained below. Each curve was shifted with respect to the curve closest to it in temperature. The best fit straight line was found for each curve on the Log-Log plots. An overlap region was identified between the two curves, as

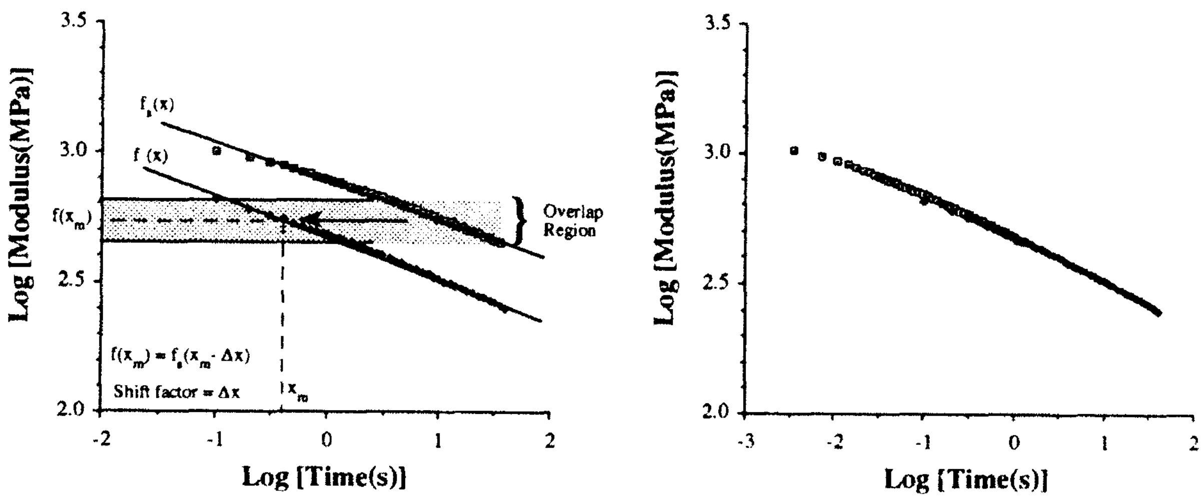

a. Relaxation Plots

b. Shifted Curve

Figure 4. Illustration of the Method of Curve Shifting

shown in Figure 4a. The midpoint of this region along the vertical axis was determined as $f(x_m)$. The shift, Δx, was then determined by solving the following equation:

$$f(x_m) = f_s(x_m - \Delta x). \tag{1}$$

If there was no curve overlap, as in some instances, the midpoint on the vertical axis between the extreme lower point of one curve and the extreme upper point of the other was used as $f(x_m)$. By shifting in this manner the shift factor is uniquely determined. The resulting combined curve is shown in Figure 4b. The advantages of this method are the definition of a unique shift factor, and the preservation of the nature of the overall curve fit, i.e., all curve segments are not forced to a single fit with the reference curve, but a relative fit with adjacent curves.

Master curves are presented in Figure 5. The master curves for M14 and M43 are fit best with a second order polynomial ($R^2 = 1.00$), which indicates multiple relaxation mechanisms are active that have different levels of activity as a function of temperature. The JA2 master curve is best fit with a linear equation ($R^2 = 0.999$) indicating that a single relaxation process dominates over the temperature range tested. The M30 master curve seems best fit with two linear curves indicating either a single mechanism operating in different material phases or two mechanisms one of which dominates at the lower temperatures (-40 to -20°C) and the other dominates at the higher (0 to 60°C). Note how the curve at 0°C nicely bridges the lower and higher temperature curves.

3.2 Shift Factors. The logarithm of the shift factors corresponding to the uncompensated master curves is plotted for each propellant in Figure 6. These plots indicate what temperature change is required in order to represent an equivalent rate change. Note that for M30 and M43 propellants the points are much better fit with a second order polynomial. Linear fits are used here to approximate the projected temperature-rate equivalence. Table 3 shows this information for each propellant, based on the linear least square fits shown. These numbers indicate that the mechanical response of materials undergoing high rates of deformation can be approximated by tests performed at lower rates and lower temperatures. Specific application of these results will be discussed in the *FUTURE STUDIES* section below.

4. CONCLUSIONS

Uniaxial stress relaxation measurements have been performed in compression on the four basic types of gun propellant. Single-, double-, and triple-based conventional propellant (M14, JA2, M30) and a nitramine composite (M43) were tested at -40, -20, 0, 20, and 60°C. The rate of compression

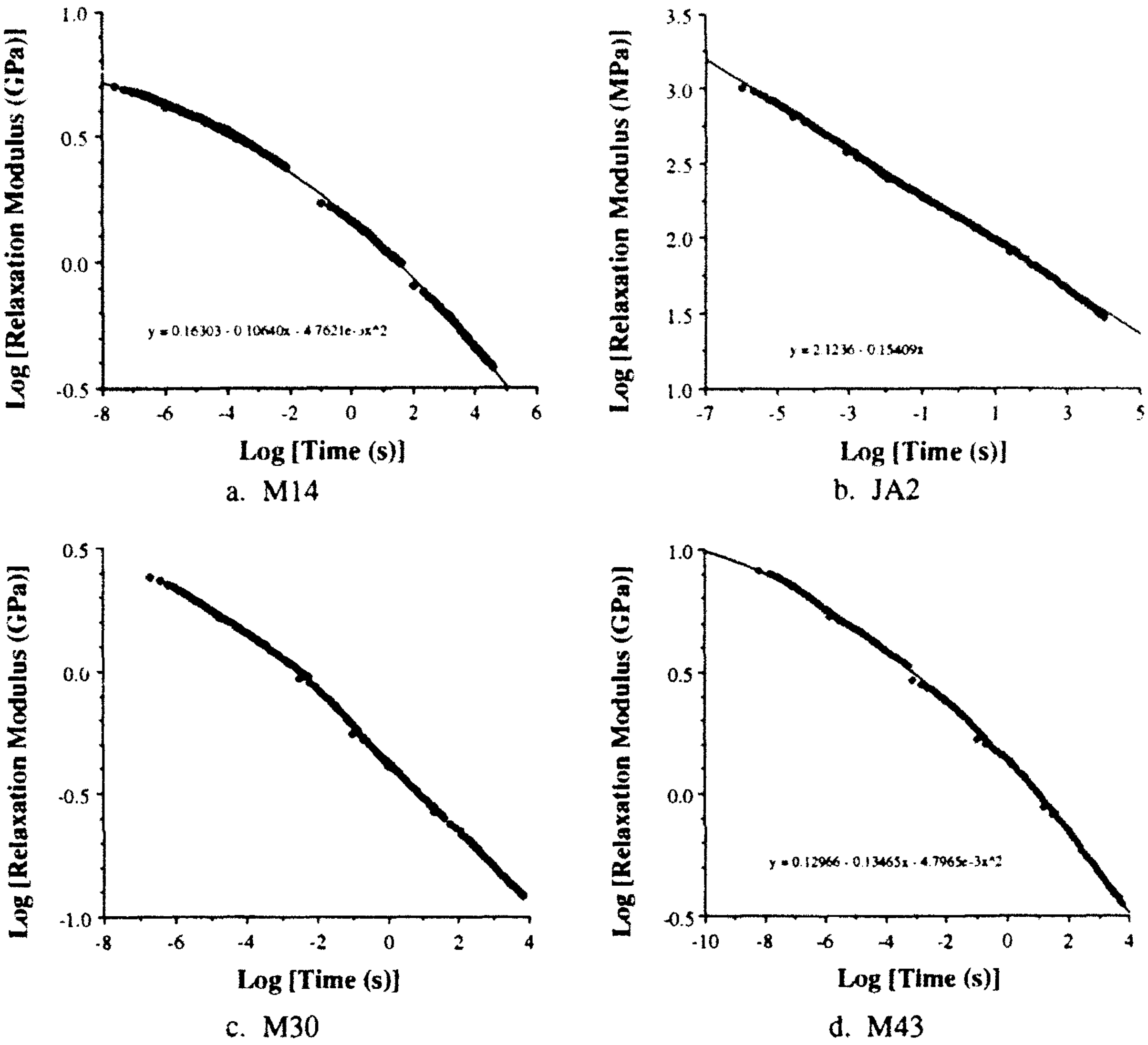

Figure 5. Master Relaxation Curves without Temperature Correction for Each Propellant

for these measurements was 1.00 s^{-1}. Master relaxation curves were generated and time-temperature shift factors were calculated. The single-based and nitramine composite propellant master curves showed a very good fit to a second order polynomial indicating multiple, competing relaxation processes. The double-based propellant master curve fit a linear curve very well indicating that a single mechanism dominates at this rate and over this temperature range. It is interesting to note that the temperature compensated master curve (discussed in Appendix I) and the uncompensated master curve closely overlap, but shift factors calculated using these curves differ significantly. The triple-based master curve showed two linear sections within the master curve indicating that different relaxation mechanisms dominate or that different phase states exist in the high (above 0°C) and the

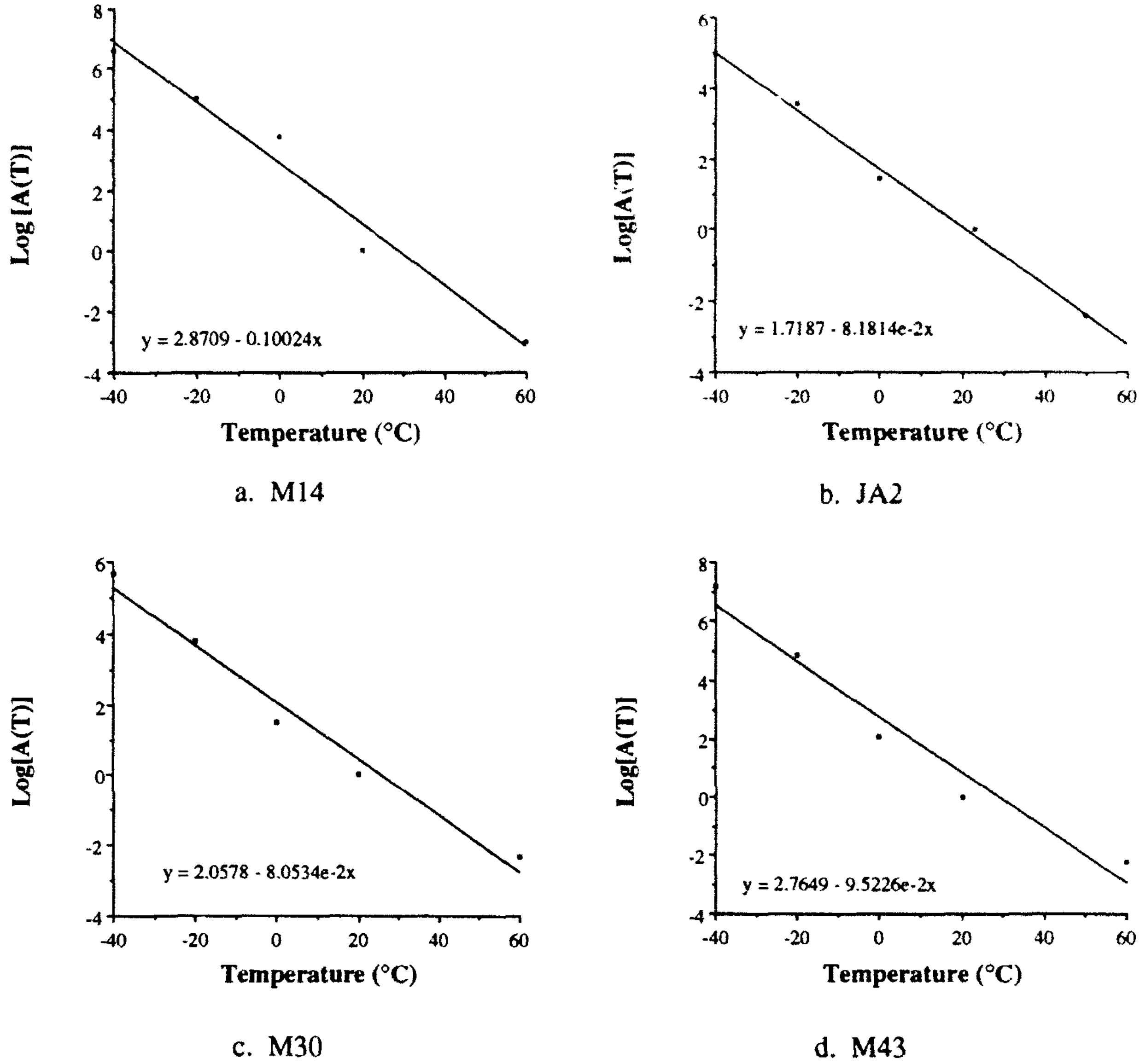

Figure 6. Shift Factors Used to Generate the Uncorrected Master Relaxation Curves

low (below -20°C) temperature regions. The shift factors that generated these master curves showed that the propellants had similar time-temperature equivalence (within about 20%). However, the possibility of some propellant grouping exists, since the propellants that showed a good quadratic fit averaged lower temperature change per decade of rate change, whereas the propellants that showed more linear fitting showed a higher rate per decade. Presently, no assessment has been made as to the significance of this observation.

Table 3. Time-Temperature Equivalence

Propellant	Fit Slope ($°C^{-1}$)	ΔT per Decade (°C per Decade)
M14	0.1002	9.98
JA2	0.0818	12.2
M30	0.0805	12.4
M43	0.0952	10.5

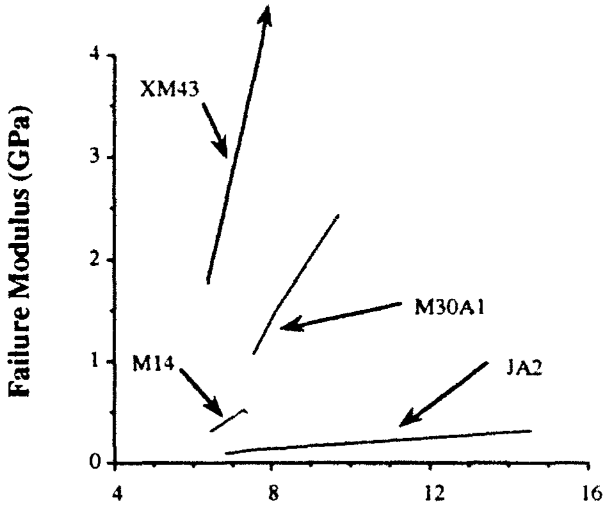

Figure 7. Failure Modulus vs the SCJ Propellant Bed Response

5. FUTURE STUDIES

In earlier studies[2,3] a strong correlation was discovered between the change in the mechanical failure response of the propellants studied in this paper and the vulnerability response change that was measured when beds of these propellants were subjected to hypervelocity impact by a shaped charge jet (SCJ). Each propellant showed a similar trend between the failure parameter and impulse measurement, which indicated a SCJ response dependence on the mechanical failure mechanisms. However, there was no direct correlation between the values of the failure parameters and the impulse results among the propellants. Figure 7 shows the relationship between the two responses at lower temperatures. One possible reason for not being able to discover a direct correlation could be due to the rate differences experienced by the propellants in the mechanical properties and the hypervelocity impact procedures.

It is estimated that the rate of deformation of the propellant while being deformed by the jet is between 10^4 and 10^6 s^{-1}. The mechanical response measurements take place at 100 s^{-1}. The rate difference between the two processes corresponds to a factor between 10^2 and 10^4. With the information generated in this report, each propellant could be tested at a temperature appropriately selected to reveal how well the mechanical response tracks with the vulnerability response when deformed under more equivalent conditions

Before the testing outlined above is performed, however, the equivalency of the response should be demonstrated as a check of the predictions and to see to what extent the equivalency of the response extends. This could be accomplished by measuring the mechanical response at temperature-rate combinations that are predicted to be equivalent over several decades of rate. A comparison of the response and parameters calculated from this response should reveal how well this application of time-temperature superposition will work.

When the above work is completed, the information generated should help make the role that mechanical response plays in the area of vulnerability response clearer. Tests are now scheduled for these propellants and will be reported.

6. REFERENCES

1. G. A. Gazonas, A. Juhasz, and J. C. Ford, "Strain Rate Insensitivity of Damaged-Induced Surface Area in M30 and JA2 Gun Propellants," BRL-TR-3251, US Army Ballistic Research Laboratory, Aberdeen Proving Ground, Maryland, August 1991.

2. P. Lu, B. Strauss, S. Moy, and R. Lieb. "Shaped Charge Jet Impact on Gun Propellants Study I - Temperature and Mechanical Properties Effects," 1991 Propulsion System Hazards Subcommittee Meeting, CPIA Publication 562, pp 517-531, March 1991.

3. R. J. Lieb, and M. G. Leadore, "Mechanical Failure Parameters in Gun Propellants," BRL-TR-3296, US Army Ballistic Research Laboratory, Aberdeen Proving Ground, Maryland, November 1991.

4. J. D. Ferry, Viscoelastic Properties of Polymers, Wiley, New York, 1961, pp 201-210.

5. J. J. Aklonis, W. J. MacKnight, and M. Shen, Introduction to Polymer Viscoelasticity, Wiley-Interscience, New York, 1972, pp 46-55.

6. G. A. Gazonas, "The Mechanical Response of M30, XM39, and JA2 Propellants at Strain Rates from 10^{-2} to 250 s^{-1}." BRL-TR-3181, USA Ballistic Research Laboratory, Aberdeen Proving Ground, Maryland, January 1991.

INTENTIONALLY LEFT BLANK.

APPENDIX A

Temperature Corrected Master Curves

INTENTIONALLY LEFT BLANK.

The mechanical behavior of materials can be projected at higher or lower strain rates by shifting the relaxation curves that have been reported here through the procedure outlined in Section IV of this report. If these shifted curves are to be used to predict the response characteristics at the reference temperature, then temperature and density (ρ) corrections need to be made. Ferry[4] states that to predict response characteristics at a temperature, T, other than the reference temperature, T_r, from a master curve, a shift of $\text{Log}(\rho T/\rho_r T_r)$ is required. Therefore, in order to construct a master curve from data taken at different temperatures, relaxation modulus values must be shifted vertically by $\text{Log}(\rho_r T_r/\rho T)$ before the separate pieces can be shifted horizontally to create the master curve.

Since density differences are very small, only the temperature corrections were made in the construction of the master curve at a reference temperature of 20°C. These curves for each propellant are shown in Figure A1, below. Note that the general shape of the curves has not changed from those found for the uncorrected master curves (Figure 4) presented earlier.

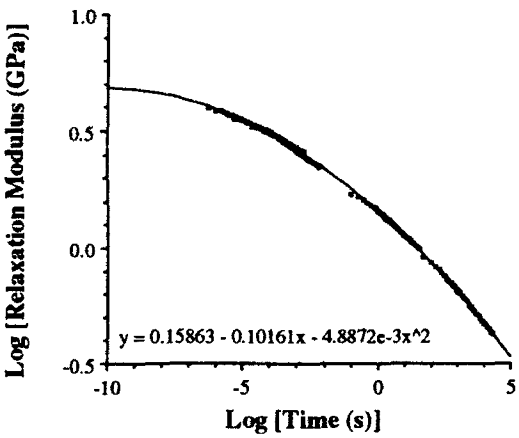

a. M14

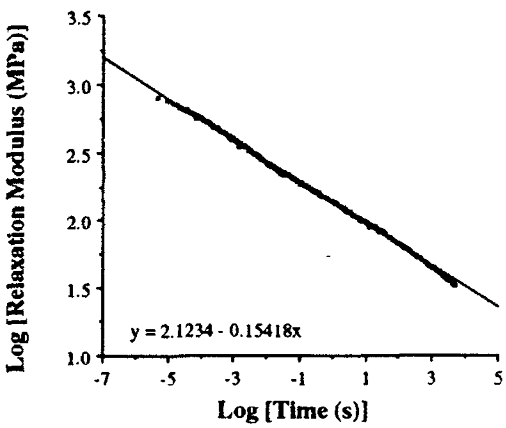

b. JA2

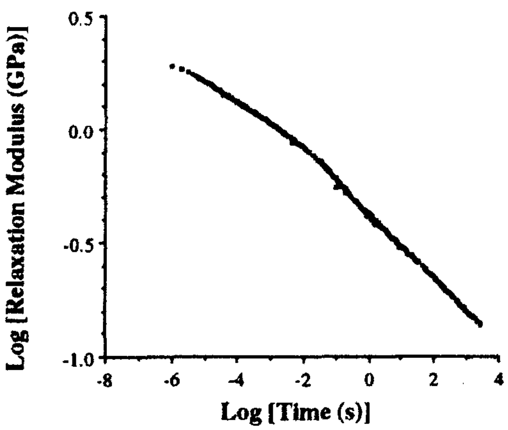

c. M30

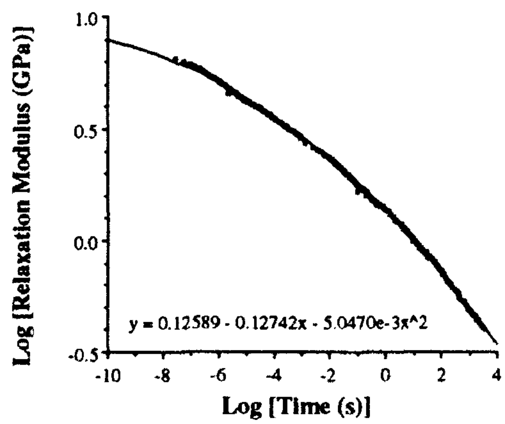

d. M43

Figure A1. Master Relaxation Curves for Each Propellant

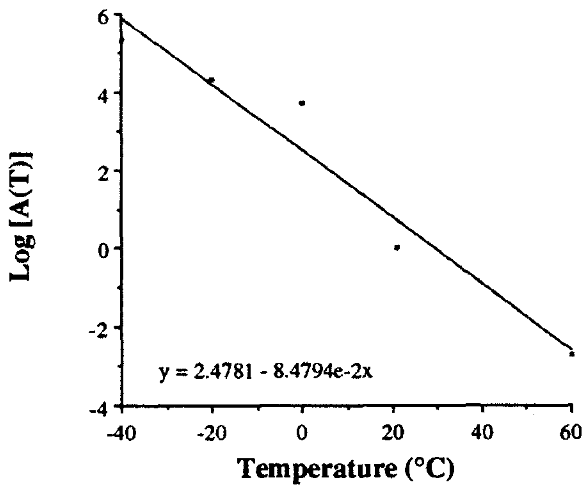

a. M14

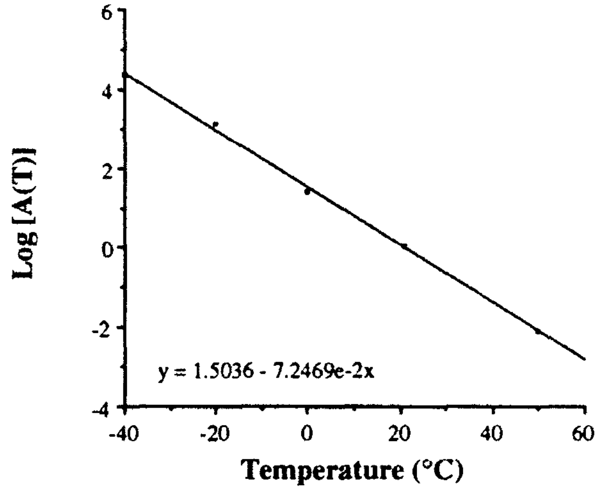

b. JA2

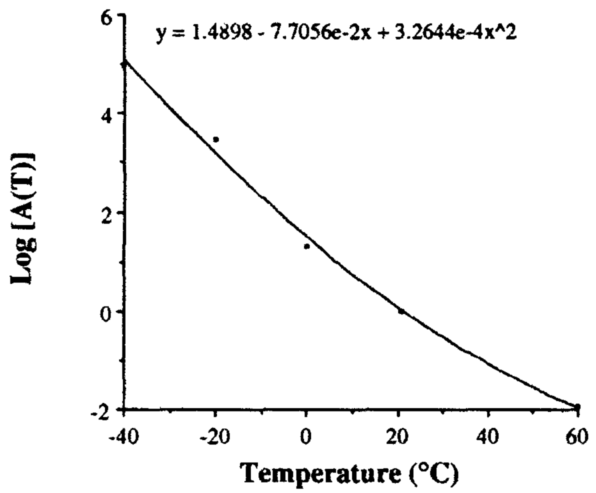

c. M30

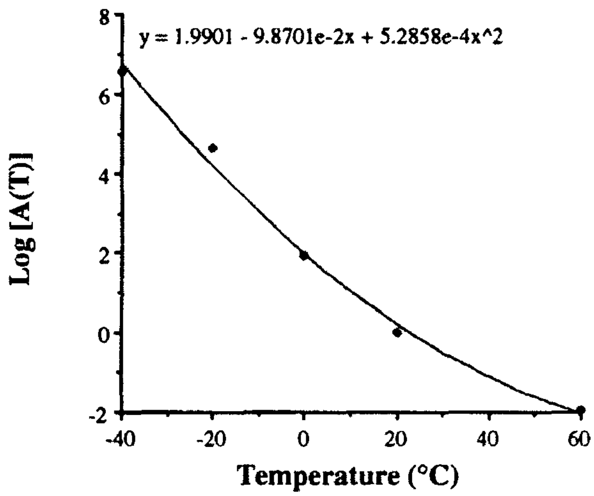

d. M43

Figure A2. Shift Factors Used to Generate the Master Relaxation Curves

It should be noted that the temperature correction shift is usually small, and is sometimes ignored when creating master curves. However, the degree to which this correction affects the value of Log[A(T)] depends on the slope of the relaxation curve segments. The closer the slope is to zero, the more the value of the corrected Log[A(T)] value is affected. Figure A2 shows the values of Log[A(T)] plotted against temperature for each of the propellants. These values were calculated from the shifted curves. To provide a comparison of the values derived from the corrected and uncorrected relaxation curves, the values of Log[A(T)] used to create both master curves are listed in Table A1 for each propellant.

Table A1. Comparison of the Values of Log[A(T)] Used to Shift the Uncorrected and Temperature Corrected Relaxation Curves

T	M14		JA2		M30		M43	
(°C)	Uncor.	Cor	Uncor.	Cor	Uncor.	Cor	Uncor.	Cor
-40	6.60	5.30	4.94	4.34	5.69	4.98	7.17	6.56
-20	5.00	4.31	3.55	3.13	3.79	3.45	4.86	4.62
0	3.75	3.70	1.45	1.36	1.51	1.31	2.09	1.92
20	0	0	0*	0*	0	0	0	0
60	-2.98	-2.70	- 2.41*	-2.11*	-2.31	-1.94	-2.20	-1.95

* JA2 temperatures were -40°C, -20°C, 0°C, 23°C and 50°C

INTENTIONALLY LEFT BLANK.

No. of Copies	Organization
2	Administrator Defense Technical Info Center ATTN: DTIC-DDA Cameron Station Alexandria, VA 22304-6145
1	Commander U.S. Army Materiel Command ATTN: AMCAM 5001 Eisenhower Ave. Alexandria, VA 22333-0001
1	Director U.S. Army Research Laboratory ATTN: AMSRL-OP-CI-AD, Tech Publishing 2800 Powder Mill Rd. Adelphi, MD 20783-1145
1	Director U.S. Army Research Laboratory ATTN: AMSRL-OP-CI-AD, Records Management 2800 Powder Mill Rd. Adelphi, MD 20783-1145
2	Commander U.S. Army Armament Research, Development, and Engineering Center ATTN: SMCAR-IMI-I Picatinny Arsenal, NJ 07806-5000
2	Commander U.S. Army Armament Research, Development, and Engineering Center ATTN: SMCAR-TDC Picatinny Arsenal, NJ 07806-5000
1	Director Benet Weapons Laboratory U.S. Army Armament Research, Development, and Engineering Center ATTN: SMCAR-CCB-TL Watervliet, NY 12189-4050
(Unclass. only) 1	Commander U.S. Army Rock Island Arsenal ATTN: SMCRI-IMC-RT/Technical Library Rock Island, IL 61299-5000
1	Director U.S. Army Aviation Research and Technology Activity ATTN: SAVRT-R (Library) M/S 219-3 Ames Research Center Moffett Field, CA 94035-1000

No. of Copies	Organization
1	Commander U.S. Army Missile Command ATTN: AMSMI-RD-CS-R (DOC) Redstone Arsenal, AL 35898-5010
1	Commander U.S. Army Tank-Automotive Command ATTN: ASQNC-TAC-DIT (Technical Information Center) Warren, MI 48397-5000
1	Director U.S. Army TRADOC Analysis Command ATTN: ATRC-WSR White Sands Missile Range, NM 88002-5502
1	Commandant U.S. Army Field Artillery School ATTN: ATSF-CSI Ft. Sill, OK 73503-5000
(Class. only) 1	Commandant U.S. Army Infantry School ATTN: ATSH-CD (Security Mgr.) Fort Benning, GA 31905-5660
(Unclass. only) 1	Commandant U.S. Army Infantry School ATTN: ATSH-CD-CSO-OR Fort Benning, GA 31905-5660
1	WL/MNOI Eglin AFB, FL 32542-5000
	Aberdeen Proving Ground
2	Dir USAMSAA ATTN: AMXSY-D AMXSY-MP, H. Cohen
1	Cdr, USATECOM ATTN: AMSTE-TC
1	Dir, ERDEC ATTN: SCBRD-RT
1	Cdr, CBDA ATTN: AMSCB-CI
1	Dir, USARL ATTN: AMSRL-SL-I
10	Dir, USARL ATTN: AMSRL-OP-CI-B (Tech Lib)

No. of Copies	Organization
1	Chairman DOD Explosives Safety Board Room 856-C Hoffman Bldg. 1 2461 Eisenhower Avenue Alexandria, VA 22331-0600
1	Headquarters U.S. Army Materiel Command ATTN: AMCICP-AD, M. Fisette 5001 Eisenhower Ave. Alexandria, VA 22333-0001
1	U.S. Army Ballistic Missile Defense Systems Command Advanced Technology Center P.O. Box 1500 Huntsville, AL 35807-3801
1	Department of the Army Office of the Product Manager 155mm Howitzer M109A6, Paladin ATTN: SFAE-AR-HIP-IP, Mr. R. De Kleine Picatinny Arsenal, NJ 07806-5000
3	Project Manager Advanced Field Artillery System ATTN: SFAE-ASM-AF-E LTC D. Ellis T. Kuriata J. Shields Picatinny Arsenal, NJ 07801-5000
1	Project Manager Advanced Field Artillery System ATTN: SFAE-ASM-AF-Q, W. Warren Picatinny Arsenal, NJ 07801-5000
2	Commander Production Base Modernization Agency U.S. Army Armament Research, Development, and Engineering Center ATTN: AMSMC-PBM, A. Siklosi AMSMC-PBM-E, L. Laibson Picatinny Arsenal, NJ 07806-5000
4	PEO-Armaments Project Manager Tank Main Armament System ATTN: AMCPM-TMA AMCPM-TMA-105 AMCPM-TMA-120 AMCPM-TMA-AS, H. Yuen Picatinny Arsenal, NJ 07806-5000
4	Commander U.S. Army Armament Research, Development, and Engineering Center ATTN: SMCAR-CCH-V, C. Mandala E. Fennell SMCAR-CCH-T, L. Rosendorf SMCAR-CCS Picatinny Arsenal, NJ 07806-5000
19	Commander U.S. Army Armament Research, Development, and Engineering Center ATTN: SMCAR-AEE, J. Lannon SMCAR-AEE-B, A. Beardell D. Downs S. Einstein S. Westley S. Bernstein J. Rutkowski B. Brodman P. O'Reilly R. Cirincione A. Grabowsky P. Hui J. O'Reilly SMCAR-AEE-WW, M. Mezger J. Pinto D. Wiegand P. Lu C. Hu SMCAR-AES, S. Kaplowitz Picatinny Arsenal, NJ 07806-5000
1	Commander U.S. Army Armament Research, Development and Engineering Center ATTN: SMCAR-HFM, E. Barrieres Picatinny Arsenal, NJ 07806-5000

No. of Copies	Organization
9	Commander U.S. Army Armament Research, Development and Engineering Center ATTN: SMCAR-FSA-T, M. Salsbury SMCAR-FSA-F, LTC R. Riddle SMCAR-FSC, G. Ferdinand SMCAR-FS, T. Gora SMCAR-FS-DH, J. Feneck SMCAR-FSS-A, R. Kopman B. Machek L. Pinder SMCAR-FSN-N, K. Chung Picatinny Arsenal, NJ 07806-5000
3	Director Benet Weapons Laboratories ATTN: SMCAR-CCB-RA, G.P. O'Hara G.A. Pflegl SMCAR-CCB-S, F. Heiser Watervliet, NY 12189-4050
2	Commander U.S. Army Research Office ATTN: Technical Library D. Mann P.O Box 12211 Research Triangle Park, NC 27709-2211
1	Commander, USACECOM R&D Technical Library ATTN: ASQNC-ELC-IS-L-R, Myer Center Fort Monmouth, NJ 07703-5301
1	Director U.S. Army Research Laboratory ATTN: AMSRL-D 2800 Powder Mill Rd. Adelphi, MD 20783-1145
1	Commandant U.S. Army Aviation School ATTN: Aviation Agency Fort Rucker, AL 36360
1	Program Manager U.S. Tank-Automotive Command ATTN: AMCPM-ABMS, T. Dean Warren, MI 48092-2498

No. of Copies	Organization
1	Project Manager U.S. Tank-Automotive Command Fighting Vehicle Systems ATTN: SFAE-ASM-BV Warren, MI 48397-5000
1	Project Manager, Abrams Tank System ATTN: SFAE-ASM-AB Warren, MI 48397-5000
1	Director HQ, TRAC RPD ATTN: ATCD-MA Fort Monroe, VA 23651-5143
1	Commander U.S. Army Belvoir Research and Development Center ATTN: STRBE-WC Fort Belvoir, VA 22060-5006
1	Director U.S. Army TRAC-Ft. Lee ATTN: ATRC-L, Mr. Cameron Fort Lee, VA 23801-6140
1	Commandant U.S. Army Command and General Staff College Fort Leavenworth, KS 66027
1	Commandant U.S. Army Special Warfare School ATTN: Rev and Trng Lit Div Fort Bragg, NC 28307
1	Commander Radford Army Ammunition Plant ATTN: SMCAR-QA/HI LIB Radford, VA 24141-0298
1	Commander U.S. Army Foreign Science and Technology Center ATTN: AMXST-MC-3 220 Seventh Street, NE Charlottesville, VA 22901-5396

No. of Copies	Organization
2	Commandant U.S. Army Field Artillery Center and School ATTN: ATSF-CO-MW, E. Dublisky ATSF-CN, P. Gross Ft. Sill, OK 73503-5600
1	Commandant U.S. Army Armor School ATTN: ATZK-CD-MS, M. Falkovitch Armor Agency Fort Knox, KY 40121-5215
1	U.S. Army European Research Cffice ATTN: Dr. Roy E. Richenbach Box 65 FPO New York 09510-1500
2	Commander Naval Sea Systems Command ATTN: SEA 62R SEA 64 Washington, DC 20362-5101
1	Commander Naval Air Systems Command ATTN: AIR-954-Tech Library Washington, DC 20360
4	Commander Naval Research Laboratory ATTN: Technical Library Code 4410, K. Kailasanate J. Boris E. Oran Washington, DC 20375-5000
1	Office of Naval Research ATTN: Code 473, R.S. Miller 800 N. Quincy Street Arlington, VA 22217-9999
1	Office of Naval Technology ATTN: ONT-213, D. Siegel 800 N. Quincy St. Arlington, VA 22217-5000

No. of Copies	Organization
3	Commander Naval Surface Warfare Center ATTN: Code 730 Code R-13, R. Bernecker H. Sandusky Silver Spring, MD 20903-5000
7	Commander Naval Surface Warfare Center ATTN: T.C. Smith K. Rice S. Mitchell S. Peters J. Consaga C. Gotzmer Technical Library Indian Head, MD 20640-5000
4	Commander Naval Surface Warfare Center ATTN: Code G30, Guns & Munitions Div Code G32, Guns Systems Div Code G33, T. Doran Code E23 Technical Library Dahlgren, VA 22448-5000
5	Commander Naval Air Warfare Center ATTN: Code 388, C.F. Price T. Boggs Code 3895, T. Parr R. Derr Information Science Division China Lake, CA 93555-6001
1	Commanding Officer Naval Underwater Systems Center ATTN: Code 5B331, Technical Library Newport, RI 02840
1	AFOSR/NA ATTN: J. Tishkoff Bolling AFB, D.C. 20332-6448
1	OLAC PL/TSTL ATTN: D. Shiplett Edwards AFB, CA 93523-5000

No. of Copies	Organization
3	AL/LSCF ATTN: J. Levine L. Quinn T. Edwards Edwards AFB, CA 93523-5000
1	WL/MNAA ATTN: B. Simpson Eglin AFB, FL 32542-5434
1	WL/MNME Energetic Materials Branch 2306 Perimeter Rd. STE 9 Eglin AFB, FL 32542-5910
1	WL/MNSH ATTN: R. Drabczuk Eglin AFB, FL 32542-5434
2	NASA Langley Research Center ATTN: M.S. 408, W. Scallion D. Witcofski Hampton, VA 23605
1	Central Intelligence Agency Office of the Central References Dissemination Branch Room GE-47, HQS Washington, DC 20502
1	Central Intelligence Agency ATTN: J. Backofen NHB, Room 5N01 Washington, DC 20505
1	SDIO/TNI ATTN: L.H. Caveny Pentagon Washington, DC 20301-7100
1	SDIO/DA ATTN: E. Gerry Pentagon Washington, DC 21301-7100
2	HQ DNA ATTN: D. Lewis A. Fahey 6801 Telegraph Rd. Alexandria, VA 22310-3398

No. of Copies	Organization
1	Director Sandia National Laboratories Energetic Materials & Fluid Mechanics Department, 1512 ATTN: M. Baer P.O. Box 5800 Albuquerque, NM 87185
1	Director Sandia National Laboratories Combustion Research Facility ATTN: R. Carling Livermore, CA 94551-0469
4	Director Lawrence Livermore National Laboratory ATTN: L-355, A. Buckingham G. Benedetti M. Finger L-324, M. Constantino P.O. Box 808 Livermore, CA 94550-0622
2	Director Los Alamos Scientific Lab ATTN: T3/D. Butler M. Division/B. Craig P.O. Box 1663 Los Alamos, NM 87544
2	Battelle ATTN: TACTEC Library, J.N. Huggins V. Levin 505 King Avenue Columbus, OH 43201-2693
1	Battelle PNL ATTN: Mr. Mark Garnich P.O. Box 999 Richland, WA 99352
1	Institute of Gas Technology ATTN: D. Gidaspow 3424 S. State Street Chicago, IL 60616-3896
1	Institute for Advanced Technology ATTN: T.M. Krehne The University of Texas of Austin 4030-2 W. Braker Lane Austin, TX 78759-5329

No. of Copies	Organization
2	CPIA - JHU ATTN: Hary J. Hoffman T. Christian 10630 Little Patuxent Parkway Suite 202 Columbia, MD 21044-3200
1	Brigham Young University Department of Chemical Engineering ATTN: M. Beckstead Provo, UT 84601
1	Jet Propulsion Laboratory California Institute of Technology ATTN: L.D. Strand, MS 125/224 4800 Oak Grove Drive Pasadena, CA 91109
1	California Institute of Technology 204 Karman Lab Main Stop 301-46 ATTN: F.E.C. Culick 1201 E. California Street Pasadena, CA 91109
3	Georgia Institute of Technology School of Aerospace Engineering ATTN: B.T. Zim E. Price W.C. Strahle Atlanta, GA 30332
1	Massachusetts Institute of Technology Department of Mechanical Engineering ATTN: T. Toong 77 Massachusetts Avenue Cambridge, MA 02139-4307
2	University of Illinois Department of Mechanical/Industry Engineering ATTN: H. Krier R. Beddini 144 MEB; 1206 N. Green St. Urbana, IL 61801-2978
1	University of Maryland ATTN: Dr. J.D. Anderson College Park, MD 20740

No. of Copies	Organization
1	University of Massachusetts Department of Mechanical Engineering ATTN: K. Jakus Amherst, MA 01002-0014
1	University of Minnesota Department of Mechanical Engineering ATTN: E. Fletcher Minneapolis, MN 55414-3368
3	Pennsylvania State University Department of Mechanical Engineering ATTN: V. Yang K. Kuo C. Merkle University Park, PA 16802-7501
1	Rensselaer Polytechnic Institute Department of Mathematics Troy, NY 12181
1	Stevens Institute of Technology Davidson Laboratory ATTN: R. McAlevy III Castle Point Station Hoboken, NJ 07030-5907
1	Rutgers University Department of Mechanical and Aerospace Engineering ATTN: S. Temkin University Heights Campus New Brunswick, NJ 08903
1	University of Southern California Mechanical Engineering Department ATTN: 0HE200, M. Gerstein Los Angeles, CA 90089-5199
1	University of Utah Department of Chemical Engineering ATTN: A. Baer Salt Lake City, UT 84112-1194
1	Washington State University Department of Mechanical Engineering ATTN: C.T. Crowe Pullman, WA 99163-5201
1	AFELM, The Rand Corporation ATTN: Library D 1700 Main Street Santa Monica, CA 90401-3297

No. of Copies	Organization
1	Arrow Technology Associates, Inc. ATTN: W. Hathaway P.O. Box 4218 South Burlington, VT 05401-0042
3	AAI Corporation ATTN: J. Hebert J. Frankle D. Cleveland P.O. Box 126 Hunt Valley, MD 21030-0126
2	Alliant Techsystems, Inc. ATTN: R.E. Tompkins J. Kennedy 7225 Northland Dr. Brooklyn Park, MN 55428
1	AVCO Everett Research Laboratory ATTN: D. Stickler 2385 Revere Beach Parkway Everett, MA 02149-5936
1	General Applied Sciences Lab ATTN: J. Erdos 77 Raynor Ave. Ronkonkama, NY 11779-6649
1	General Electric Company Tactical System Department ATTN: J. Mandzy 100 Plastics Ave. Pittsfield, MA 01201-3698
1	IITRI ATTN: M.J. Klein 10 W. 35th Street Chicago, IL 60616-3799
4	Hercules, Inc. Radford Army Ammunition Plant ATTN: L. Gizzi D.A. Worrell W.J. Worrell C. Chandler Radford, VA 24141-0299
2	Hercules, Inc. Allegheny Ballistics Laboratory ATTN: William B. Walkup Thomas F. Farabaugh P.O. Box 210 Rocket Center, WV 26726

No. of Copies	Organization
1	Hercules, Inc. Aerospace ATTN: R. Cartwright 100 Howard Blvd. Kenville, NJ 07847
1	Hercules, Inc. Hercules Plaza ATTN: B.M. Riggleman Wilmington, DE 19894
1	MBR Research Inc. ATTN: Dr. Moshe Ben-Reuven 601 Ewing St., Suite C-22 Princeton, NJ 08540
1	Olin Corporation Badger Army Ammunition Plant ATTN: F.E. Wolf Baraboo, WI 53913
3	Olin Ordnance ATTN: E.J. Kirschke A.F. Gonzalez D.W. Worthington P.O. Box 222 St. Marks, FL 32355-0222
1	Olin Ordnance ATTN: H.A. McElroy 10101 9th Street, North St. Petersburg, FL 33716
1	Paul Gough Associates, Inc. ATTN: P.S. Gough 1048 South St. Portsmouth, NH 03801-5423
1	Physics International Library ATTN: H. Wayne Wampler P.O. Box 5010 San Leandro, CA 94577-0599
2	Princeton Combustion Research Laboratories, Inc. ATTN: N. Mer N.A. Messina Princeton Corporate Plaza 11 Deerpark Dr., Bldg IV, Suite 119 Monmouth Junction, NJ 08852

No. of Copies	Organization
3	Rockwell International Rocketdyne Division ATTN: BA08, J. Flanagan J. Gray R.B. Edelman 6633 Canoga Avenue Canoga Park, CA 91303-2703
2	Rockwell International Science Center ATTN: Dr. S. Chakravarthy Dr. S. Palaniswamy 1049 Camino Dos Rios P.O. Box 1085 Thousand Oaks, CA 91360
1	Southwest Research Institute ATTN: J.P. Riegel 6220 Culebra Road P.O. Drawer 28510 San Antonio, TX 78228-0510
1	Sverdrup Technology, Inc. ATTN: Dr. John Deur 2001 Aerospace Parkway Brook Park, OH 44142
3	Thiokol Corporation Elkton Division ATTN: R. Willer R. Biddle Tech Library P.O. Box 241 Elkton, MD 21921-0241

No. of Copies	Organization
1	Veritay Technology, Inc. ATTN: E. Fisher 4845 Millersport Hwy. East Amherst, NY 14501-0305
1	Universal Propulsion Company ATTN: H.J. McSpadden 25401 North Central Ave. Phoenix, AZ 85027-7837
1	SRI International Propulsion Sciences Division ATTN: Tech Library 333 Ravenwood Avenue Menlo Park, CA 94025-3493
	Aberdeen Proving Ground
1	Cdr, USACSTA ATTN: STECS-PO/R. Hendricksen

No. of Copies	Organization
1	Ernst-Mach-Institut ATTN: Dr. R. Heiser Haupstrasse 18 Weil am Rheim Germany
1	Defence Research Agency, Military Division ATTN: C. Woodley RARDE Fort Halstead Sevenoaks, Kent, TN14 7BP England
1	School of Mechanical, Materials, and Civil Engineering ATTN: Dr. Bryan Lawton Royal Military College of Science Shrivenham, Swindon, Wiltshire, SN6 8LA England

No. of Copies	Organization
2	Institut Saint Louis ATTN: Dr. Marc Giraud Dr. Gunther Sheets Postfach 1260 7858 Weail am Rhein 1 Germany
1	Explosive Ordnance Division ATTN: A. Wildegger-Gaissmaier Defence Science and Technology Organisation P.O. Box 1750 Salisbury, South Australia 5108
1	Armaments Division ATTN: Dr. J. Lavigne Defence Research Establishment Valcartier 2459, Pie XI Blvd., North P.O. Box 8800 Courcelette, Quebec G0A 1R0 Canada